Journal of Nuclear Materials 390–391 (2009) 626–630

Contents lists available at ScienceDirect

Journal of Nuclear Materials

journal homepage: www.elsevier.com/locate/jnucmat

Thermo-oxidation and analysis of JET codeposits

A.A. Haasz [a,*], J. Likonen [b], J.P. Coad [c], C.K. Tsui [a], J.W. Davis [a], A.M. Widdowson [c]

[a] University of Toronto Institute for Aerospace Studies, 4925 Dufferin St., Toronto, ON, Canada M3H5T6
[b] Association EURATOM-TEKES, VTT Processes, P.O. Box 1000, 02044 VTT, Espoo, Finland
[c] Culham Science Centre, EURATOM/UKAEA-Fusion Association, Abingdon, Oxfordshire, OX14 3DB, UK

ARTICLE INFO

PACS:
28.52.Fa
81.05.Uw
81.65.Mq
82.45.Mp

ABSTRACT

Following the thermo-oxidation study of D removal from JET divertor codeposits, post oxidation surface analyses were performed using SIMS, NRA and profilometry. The analysis confirms that the D content was reduced by at least an order of magnitude after 8-h oxidation at 623 K (350 °C) and 21 kPa (160 Torr) O_2 pressure – in agreement with TDS measurements. The codeposits studied contain Be and C. Those on the vertical tile surfaces have a duplex structure with a C-D rich layer on the surface and a Be–C layer underneath; during oxidation the outer layer is removed and the inner layer remains. Codeposits with low Be content from the shadowed area have single-layer structures; during oxidation their thicknesses were reduced by about an order of magnitude. For the JET codeposits studied (with Be/C up to ~1) it appears that Be does not affect the oxidative removal of deuterium from the codeposit in a significant way.

1. Introduction

Thermo-oxidation in air or mixtures of O_2 with inert gases is one of the techniques being developed for the recovery of tritium from tokamak codeposits. Earlier oxidation studies include D removal from laboratory-produced a-C:H films [1–3] and tokamak codeposits from TFTR [4–6], ASDEX-U [3], JET [6,7], DIII-D [6–8] and TEXTOR [9]. More recently, thermo-oxidation was performed on thick JET divertor codeposits (10–250 μm) with Be/C ratio up to ~1 [10]. Two key findings were reported: (i) For oxidation at 350 °C and 21 kPa O_2 pressure, D removal from the JET codeposits [10] occurs much more rapidly than from the thinner tokamak codeposits [7,8]. The D release rate varies linearly with the initial D concentration, i.e., the more inherent D is in the codeposit, the faster it is released. (ii) D removal rates were not affected by the presence of Be. Based on these observations it was suggested that D removal during oxidation occurs throughout the codeposit, and not by progressive recession of the geometric surface [10].

The present study was undertaken to investigate the changes in the elemental composition and structure of the codeposits following oxidation – by performing post-oxidation surface analysis and depth profiling on the oxidized JET specimens used in [10]. To explore the evolution of the codeposited layer during oxidation, new experiments were performed for 15-min oxidation periods, which were again analysed by SIMS and NRA. The reader is referred to [10] for background information relevant to the present study.

2. Codeposit specimens and oxidation experiment

We used two sets of codeposits cut from tiles 1, 3 and 4 of the JET Mark II Gas Box divertor, which were in JET during the 1998–2001 Gas Box campaign [11]. Specimens were typically ~1 cm×2 cm. Set-1 included nine specimens used in the oxidation experiments of Tsui et al. [10]. Set-2, here referred to as 'reference specimens', came from locations right next to the respective specimens of Set-1 in the toroidal direction; no reference specimen was available for sp10 due to insufficient material from the sloping part of tile 4. (We note that the reference set provides a check on the pre-oxidation surface analysis data for Set-1 presented in Table 2 of [10]; for the most part the agreement is within a factor of ~1.5.)

The pre-oxidation D, C, and Be concentrations and thicknesses for the 'reference specimens' are given in Table 1. This reference set was subsequently oxidized – in the present study – for 15 min (at 350 °C and 21 kPa O_2 pressure) followed by another round of surface analysis. Table 1 also includes the post-oxidation analyses for the 8-h (Set-1) and 15-min (Set-2) cases. Specimen locations are shown in Fig. 1; the notation is the same as in [10]. The amount of D removed after 15-min oxidation for Set-2 is in good agreement with the results in Fig. 7 of Ref. [10] for the same oxidation time – indicating good reproducibility.

3. Post-oxidation surface analysis

Pre- and post-oxidation surface analysis included secondary ion mass spectrometry (SIMS), performed at the Technical Research Centre of Finland, VTT, and ion-beam analysis (IBA), at the University of Sussex, Brighton, UK. The primary components of these JET

* Corresponding author.
E-mail address: tonyhaasz@utias.utoronto.ca (A.A. Haasz).

0022-3115/$ - see front matter © 2009 Elsevier B.V. All rights reserved.
doi:10.1016/j.jnucmat.2009.01.303

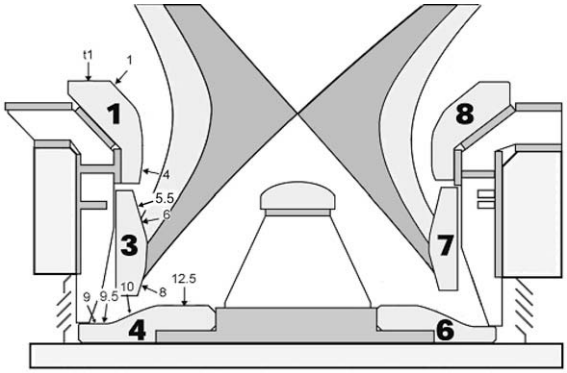

Fig. 1. Schematic of JET Mark II Gas Box divertor showing the specimen locations used for the oxidation experiments performed for this study and also in [10].

films (C, Be and D) could be analysed simultaneously using nuclear reaction analysis (NRA) through the reactions $^{12}C(^3He,p)^{14}N$, $^9Be(^3He,p)^{11}B$ and $^2D(^3He,p)^4He$; the analysis spot was ~1 mm diameter and the depth with a 2.5 MeV ^3He beam was ~1, ~2 and ~7 μm for C, Be and D, respectively. Additionally, we used Rutherford backscattering spectroscopy (RBS) with 2.5 MeV protons to check on the thicknesses and uniformity of the films, and simultaneous particle - induced X-ray emission (PIXE) analysis to check the concentrations of other metals.

For SIMS a double focussing magnetic sector instrument (VG Ionex IX-70S) was used. The secondary ions ($^1H^+$, $^2D^+$, $^9Be^+$, $^{10}B^+$, $^{12}C^+$, $^{13}C^+$, and $^{58}Ni^+$) produced by a ~500 nA 5 keV O_2^+ primary beam were profiled – over an area of 300 × 430 μm^2. Surface profilometry of a redeposited layer allowed the determination of the layer thickness and, consequently, the assessment of the sputter rates in SIMS. Relative uncertainty in the sputter rates is estimated to be ±15%.

4. Surface analysis results and discussion

Surface analyses have revealed that while most codeposits were 'single-layers', those from the vertical surfaces of tiles 1 and 3 had 'duplex' structures. The most likely reason for the duplex nature of the codeposit layers is the He-fuelling campaign for one month towards the end of the 1998–2001 Gas Box campaign in 2001 [12]. The interpretation of the NRA measurements was aided by the SIMS profiles; see examples in Fig. 2. Below we shall discuss how the structure and the concentrations were affected by oxidation. (Pre- and post-oxidation conditions are referred to as 'before' and 'after', respectively. The noted D/C reductions after 15-min and 8-h oxidation are based on the pre-oxidation reference concentrations).

4.1. Single-layer

4.1.1. Specimen spt1 (top of tile-1)

Before: ~50 μm; Be/C ~0.32; D/C ~0.05.

After 15-min: thickness unaffected but D/C reduced by ~40%.

After 8-h: thickness and Be/C unaffected, but there was some redistribution of Be and other metals within the film; D/C reduced

Table 1
NRA data for pre-oxidation (-ref entries) and post-oxidation (-15 min and -8 h entries). Also shown are NRA concentrations 'adjusted' to first micrometer depth according to ion ranges 1, 2, and 7 μm for C, Be and D, respectively. Specimen notation is the same as in [10]. (Specimens designated with -ref and -15 min are from Set-2 and those shown as -8 h are from Set-1).

(i) Tile # and specimen location	(ii) Codeposit thickness (μm)	NRA: outer layer			NRA: outer layer (adjusted)						
		(iii) 10^{22}D/m^2	(iv) 10^{22}Be/m^2	(v) 10^{22}C/m^2	(vi) col (iii)/7 10^{22}D/m^2	(vii) col (iv)/2 10^{22}Be/m^2	(viii) col (v)/1 10^{22}C/m^2	(ix) D/(Be + C)	(x) Be/(Be + C)	(xi) D/C	(xii) Be/C
Tile 1											
spt1-ref	49.5	1.96	3.51	5.47	0.28	1.76	5.47	0.039	0.24	0.051	0.32
spt1-15 min	49	0.97	3.15	4.42	0.14	1.58	4.42	0.023	0.26	0.032	0.36
spt1-8 h	49.7	0.14	3.67	5.25	0.02	1.84	5.25	0.003	0.26	0.004	0.35
sp1-ref	25.3	3.95	4.71	4.79	0.56	2.36	4.79	0.079	0.33	0.118	0.49
sp1-15 min	33	1.29	4.23	3.00	0.18	2.12	3.00	0.036	0.41	0.061	0.73
sp1-8 h	25.4	0.31	8.81	3.37	0.04	4.40	3.37	0.006	0.57	0.013	1.31
sp4-ref	21	5.70	5.07	3.73	0.81	2.54	3.73	0.130	0.40	0.218	0.68
sp4-15 min	17	1.55	6.76	2.37	0.22	3.38	2.37	0.038	0.59	0.097	1.47
sp4-8 h	5.4	0.33	3.95	3.26	0.05	1.98	3.26	0.009	0.38	0.014	0.61
Tile 3											
sp6-ref	53.7	11.6	1.76	4.73	1.66	0.88	4.73	0.296	0.16	0.351	0.19
sp6-15 min	47	2.51	2.87	5.17	0.36	1.43	5.27	0.054	0.21	0.070	0.28
sp6-8 h	42	0.16	4.67	4.78	0.02	2.34	4.78	0.003	0.33	0.005	0.49
sp8-ref	25.1	15.9	1.85	5.29	2.27	0.93	5.29	0.365	0.15	0.429	0.17
sp8-15 min	24	3.89	2.68	7.46	0.56	1.34	7.46	0.063	0.15	0.075	0.18
sp8-8 h	5.1	0.35	1.27	4.79	0.05	0.63	4.79	0.009	0.12	0.010	0.13
Tile 4											
sp9-ref	87.2	34.30	0.00	5.30	4.90	0.00	5.30	0.924	0.00	0.924	0.00
sp9-15 min	79	12.33	0.00	5.47	1.76	0.00	5.47	0.322	0.00	0.322	0.00
sp9-8 h	9.5	0.25	0.24	5.66	0.04	0.12	5.66	0.006	0.02	0.006	0.02
sp9.5-ref	41[a]	31.01	0.33	5.64	4.43	0.16	5.64	0.764	0.03	0.786	0.03
sp9.5-15 min	>125	15.1	0.45	7.12	2.15	0.23	7.12	0.293	0.03	0.302	0.03
sp9.5-8 h	4.8	0.89	0.43	5.53	0.13	0.21	5.53	0.022	0.04	0.023	0.04
sp10-ref[b]	270	5.1	2.2	6.5	0.73	1.1	6.5	0.10	0.14	0.11	1.17
sp10-15 min	n/a	0.88	3.25	6.14	0.13	1.63	6.14	0.016	0.21	0.022	0.28
sp10-8 h	n/a	0.17	2.84	5.40	0.02	1.42	5.40	0.004	0.21	0.005	0.27
sp12.5-ref	5.5	4.69	0.77	5.10	0.67	0.39	5.10	0.122	0.07	0.131	0.08
sp12.5-15 min	2.3	1.18	0.67	6.61	0.17	0.34	6.61	0.024	0.05	0.026	0.05
sp12.5-8 h	3.2	0.14	0.65	5.27	0.02	0.33	5.27	0.004	0.06	0.004	0.06

[a] Thickness estimate is based on the nearest spot value for which measurement was available [10].
[b] Values are from Ref. [10].

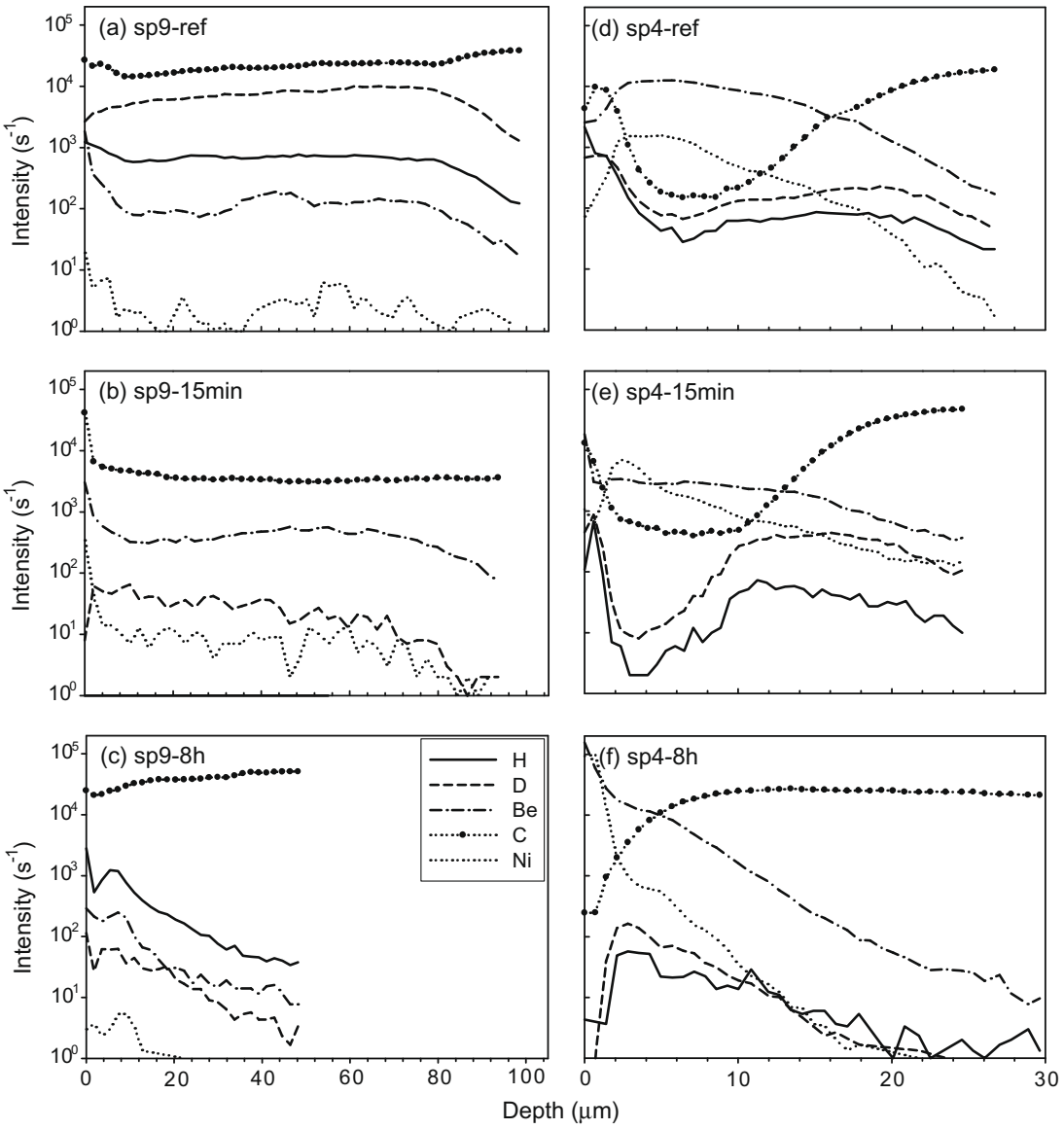

Fig. 2. Pre- and post-oxidation SIMS depth profiles: (a, b, c) 'single-layer' specimen sp9 and (d, e, f) 'duplex-structure' specimen sp4.

by a factor of 13 according to NRA; small amount of remaining D was present throughout the analysis depth, suggesting it was present in localized particles; this may explain why the SIMS profile from the oxidized specimen did not show any D.

4.1.2. Specimen sp1 (upper slanting part of tile-1)

Before: ~25 μm; Be/C ~0.5; D/C ~0.12.

After 15-min: D/C reduced by ~50%.

After 8-h: thickness unaffected; D/C reduced by a factor of ~10 with indications that the D content in some particles was difficult to reduce (also visible in the SIMS profiles); Be/C was increased to ~1.3, with indications of *discrete layers* of varying Be/C in both the SIMS profile and RBS (possibly BeC).

4.1.3. Specimen sp9 (shadowed part of tile-4)

Before: ~87 μm of almost pure C and D with D/C ~0.9.

After 15-min: thickness reduced to ~79 μm and D/C reduced by ~65%.

After 8-h: the trace D, Be and B signals suggest the film has been reduced to ~9.5 μm; D/C reduced by a factor of ~150.

4.1.4. Specimen sp9.5 (just onto the sloping part of tile-4 rather than the flat shadowed region)

Before: ~41 μm (estimate from [10]); analysis similar to that of sp9 – characteristic of the shadowed region rather than the sloping part of tile 4 where quite different film composition is expected; D/C ~0.8.

After 15-min: thickness >125 μm, implying that the pre-oxidation estimate of ~41 μm is likely to be incorrect; D/C reduced by ~60%, which confirms the results from sp9 that 15 min is not long enough to deplete the D from the codeposit in the shadowed region.

After 8-h: film thickness reduced to ~5 μm (SIMS); D/C was reduced by about a factor of 35; B and Be traces accumulated at the surface.

4.1.5. Specimen sp10 (sloping part of tile-4)

Before: due to insufficient material from this part of tile-4, the pre-oxidation thickness and concentration values listed in Table 1 are from [10]: ~270 μm thick; Be/C ~1.2; D/C ~0.11.

After 15-min: thickness not measured; D/C reduced by ~80% and Be/C reduced by ~76% to ~0.28.

After 8-h: thickness not measured; D/C was reduced by about a factor of 20 and Be/C remained at ~0.27.

4.1.6. Specimen sp12.5 (upper flat part of tile-4: not exposed to direct plasma but not shadowed from material re-sputtered from tiles 1 and 3)

Before: thin film (~5.5 μm) over the surface; D/C ~0.13; low Be content: Be/C ~0.08.

After 15-min: thickness reduced to ~2.3 μm; D/C reduced by ~80% and Be/C was reduced by ~40% to ~0.05.

After 8-h: no further thickness change; D/C reduced by a factor of ~30 with no other discernable change in the film.

4.2. Duplex structure

4.2.1. Specimen sp4 (lower vertical face of tile-1)

Before: ~20 μm; C-rich surface layer while the rest of the film has high Be/C~0.7; RBS/SIMS show that the C-rich surface layer in some areas is mostly ^{13}C (may have come from $^{13}CH_4$ puffing) where D/C ~1; in other areas ^{12}C dominates and D/C ~0.2.

After 15-min: the C–D-rich layer was still present, but thickness reduced to ~17 μm; ~55% reduction in D/C and about a factor of two increase in Be/C to ~1.5.

After8-h: this surface layer disappeared and SIMS shows a thin layer of almost pure Be plus some metals, on top of a few micrometers of more normal composition; D/C was reduced by about a factor of 15. NRA suggests again that the D removed is not uniform over the surface, with ~10% of the surface retaining some D to >7 μm, perhaps due to the presence of localized particles that resist the scavenging of D by oxygen.

4.2.2. Specimen sp6 (upper vertical part of tile-3)

Before: has a double layer – a high Be/C inner layer and a higher C and D content in an outer layer; overall thickness ~54 μm; in outermost micrometer D/C ~1 (averaged over 7 μm, D/C ~0.35); significant ^{13}C on the very surface from the puffing experiment.

After 15-min: small reduction in thickness to ~47 μm; D/C reduced by ~80%; small increase in Be/C; SIMS shows ^{13}C still present.

After 8-h: surface ^{13}C is lost; surface Be/C ~1.5; thickness decreased to ~42 μm; however, the overall two-layer structure is maintained; D/C reduced by a factor of ~70.

4.2.3. Specimen sp8 (lower vertical part of tile-3)

Before: also duplex layer, but on a reduced scale – thickness being ~25 μm; at surface D/C ~1 (averaged over 7 μm, D/C ~0.43), Be/C ~0.17, and trace of ^{13}C visible.

After 15-min: thickness and Be/C unchanged while D/C reduced by ~80%; trace of ^{13}C detected.

After 8-h: all that remains of the original film is a small amount of Be and other metals left on the surface (SIMS/RBS); D reduced by about a factor of 40 (NRA).

4.3. Changes in D, Be, and C concentrations due to thermo-oxidation

Fig. 3 shows 'adjusted' NRA-measured ratios of 'final/initial' D, Be and C concentrations as a function of initial thickness, together with the TDS-measured D ratios from [10]. It is evident from the figure that nearly all D was removed and the C content in the remaining layer was similar to that on the original surface – both within the top 1 μm surface layer. The D content of the codeposits is decreased quickly and effectively despite surface Be concentrations as high as 50% Be/(Be + C) while SIMS traces indicate higher concentrations of Be in deeper layers for some specimens. The final/initial Be concentration ratio ranges between ~0.7 and ~3, with no apparent correlation with initial codeposit thickness.

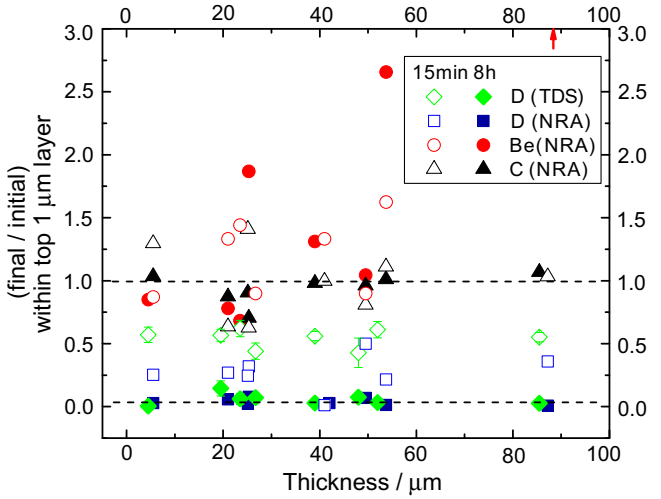

Fig. 3. NRA-measured ratios of 'removed/initial' D, Be and C concentrations ('adjusted' to the first micrometer depth according to ion ranges of 1, 2, and 7 μm for C, Be and D, respectively) as a function of initial codeposit thickness. TDS-measured D ratios from [10] are also shown. [The high Be ratio shown by ↑ for sp9 (87 μm) is due to 'near-zero' initial Be concentration].

The surface analysis does not indicate the increase in Be concentration which might be expected due to the preferential removal of carbon; i.e., similar to what was observed for boron [8]. One hypothesis is that Be or BeO particulates may be lost from the specimens during the oxidative removal of the surrounding carbon matrix. Unfortunately, safety issues associated with our tritium - containing vacuum system have limited our ability to look for such particulates. Alternatively, the expected preferential removal of carbon may not occur to the degree previously observed with B-containing codeposits [8], due to the formation of BeC; the deuterium is released, but much of the carbon remains. The formation and non-removal of BeC might also explain why, in some cases, the measured deposit thickness (SIMS) is not significantly reduced following oxidation, despite the release of the majority of the D.

Although the mechanism associated with the role of Be during oxidation cannot be identified at this time, it appears that Be does not affect the oxidative removal of deuterium from the codeposit in a significant way, in contrast to what was observed for B-containing DIII-D codeposits [8].

5. Summary and conclusions

Thermo-oxidative removal of deuterium from JET divertor codeposits was studied in [10]. Subsequently, ion-beam and SIMS analyses were performed on the oxidized specimens together with a 'reference' set to assess the changes in structure and elemental composition during oxidation. In all cases the SIMS profiles and NRA-measured D concentrations were consistent with the reported TDS data [10] – after 15-min oxidation the NRA-measured D content was reduced by about 30–50%, and after 8-h, by an order of magnitude or more. This finding is consistent with our hypothesis [10] that erosion occurs throughout the codeposit.

The codeposits had either a single-layer or duplex structure, with various concentrations of Be and C. The films on the vertical surfaces of tiles 1 and 3 were duplex with a C–D-rich outer layer and a Be-rich inner layer; following oxidation, the outer layer was removed and the Be-C layer remained. The thicknesses of the single-layer specimens with low Be content from the shadowed part of tile-4 were reduced by an order of magnitude – similar to the D reduction; Be and B traces were detected on the surface.

The ratios of 'final/initial' D, Be and C concentrations as a function of initial codeposit thickness show that nearly all D was removed and the C content in the remaining layer was similar to that on the original surface for all specimens. The Be ratio covers a wide range (0.7–3) and shows no apparent correlation with thickness. Although the mechanism associated with the role of Be during oxidation cannot be identified at this time, it appears that Be does not affect the oxidative removal of deuterium from the codeposit in a significant way, but it may affect the removal of carbon.

Implication for ITER: Assuming that ITER codeposits will have similar structure and impurity content as the JET tiles, we would expect that thermo-oxidation at ~623 K (350 °C) and 21 K Pa (160 torr) O_2 pressure would remove ~90% of the inherent D content within a day – independent of codeposit thickness and the Be content. In the case of C-rich codeposits, the majority of the layer will be eroded; in the case of C–Be mixed codeposits, some Be–C residue will remain.

Acknowledgments

The research performed at the University of Toronto was supported by the Natural Sciences and Engineering Research Council of Canada. We thank Charles Perez for his diligent work in commissioning the experimental facility. The work performed in the EU was conducted under the European Fusion Development Agreement and was partly funded by EURATOM, the UK Engineering and Physical Sciences Research Council, and the National Technology Agency of Finland.

References

[1] A.A. Haasz, S. Chiu, J.E. Pierre, Y.I. Gudimenko, J. Vac. Sci. Technol. A14 (1996) 184.
[2] S. Alberici, H.K. Hinssen, R. Moormann, C.H. Wu, J. Nucl. Mater. 266–269 (1999) 754.
[3] W. Wang, J. Jacob, J. Roth, J. Nucl. Mater. 245 (1997) 66.
[4] R.A. Causey, W.R. Wampler, D. Walsh, J. Nucl. Mater. 176&177 (1990) 987.
[5] A.A. Haasz, J.W. Davis, J. Nucl. Mater. 256 (1998) 65.
[6] J.W. Davis, A.A. Haasz, J. Nucl. Mater. 266–269 (1999) 478.
[7] R. Ochoukov, A.A. Haasz, J.W. Davis, Phys. Scr. T124 (2006) 27.
[8] A.A. Haasz, C.K. Tsui, J.W. Davis, R. Ochoukov, Phys. Scr. T128 (2007) 55.
[9] M.J. Rubel, G. De Temmerman, G. Sergienko, et al., J. Nucl. Mater. 363–365 (2007) 877.
[10] C.K. Tsui, A.A. Haasz, J.W. Davis, J.P. Coad, J. Likonen, Nucl. Fusion. 48 (2008) 035008.
[11] J.P. Coad, J. Likonen, M. Rubel, E. Vainonen-Ahlgren, et al., Nucl. Fusion 46 (2006) 350.
[12] J. Likonen, J.P. Coad, E. Vainonen-Ahlgren, T. Renvall, et al., J. Nucl. Mater. 363–365 (2007) 190.